An informational approach to the Network Disease Hypothesis in resting state fMRI

Jaime Gomez-Ramirez, Yujie Li, Qiong Wu, Xiaoyu Tang, Jinglong Wu

Abstract Here we combine graph and information theory based approaches to understand network robustness in resting state-fMRI (R-fMRI). We calculate how the network robustness is affected upon the removal of nodes in the functional connectivity network in resting state for both young and elder subjects. We find that ... predictor of aging?

Key words: resting state fMRI, network degeneration hypothesis, Markov chain, relative entropy

1 Introduction

It has been suggested that fluctuations in the BOLD signal measured in humans in resting state, represent the neuronal activity baseline and shape spatially consistent patterns [1], [2]. These slow fluctuations in the BOLD signal found in resting subjects, are highly coherent within either structural or functional networks in the human brain. Therefore, exploring these fluctuations could lead to a better understanding of the brain's intrinsic or spontaneous neural activity. Functional correlation based on the synchrony of low-frequency blood flow fluctuations in resting state, have been identified in the sensorimotor [3], visual [4], language [5], auditory [6], dorsal and ventral attention [7] and the frontoparietal control system [8]. The systematic study of those patterns using correlation analysis techniques has identified a number of resting state networks, which are functionally relevant networks found in subjects in the absence of either goal directed-task or external stimuli.

Biomedical Engineering Laboratory, Okayama University, Japan
Autonomous Systems Laboratory, Universidad Politécnica de Madrid, Spain
e-mail: jd.gomez@upm.es

The visual identification of the overall connectivity patters in resting state functional magnetic resonance imaging (R-fMRI), has been assessed using either model-based and model-free approaches. In the former, statistical parametric maps of brain activation are built upon voxel-wise analysis location. This approach has been successful in the identification of motor networks, but it shows important limitations when the seed voxel cannot be easily identified. For example, in brain areas with unclear boundaries i.e., cognitive networks involved for instance, in language or memory. Independent Component Analysis (ICA), on the other hand, is a model-free approach that allows separating resting fluctuations from other signal variations, resulting on a collection of spatial maps, one for each independent component, that represent functionally relevant networks in the brain. While ICA has the advantage over model-free methods that it is unbiased, (that is, it does not need to posit a specific temporal model of correlation between ROIs), the functional relevance of the different components is, however, computed relative to their resemblance to a number of networks based on criteria that are not easily formalized.

More recently, researchers using graph-theory based methods have been able to not only visualize brain networks, but to quantify their topological properties. Large-scale anatomical connectivity analysis in the mammalian brain, shows that brain topology is neither random nor regular. Instead, small world architectures [9] -highly clustered nodes connected thorough relatively short paths- have been identified in brain networks. Small world networks are not solely structural, functional networks with a small world organization have been identified in the mammal brain [10]. In addition to this, disruptions in the small world organization can give clues about normal development and pathological conditions. For example, Supekar and colleagues [11] have shown that the deterioration of small world properties such as the lowering of the cluster coefficient, affect local network connectivity, which in turn may work as a network biomarker for Alzheimer's disease. Abnormalities in small-worldness may also have a significant positive correlation in, for example, schizophrenia [12] and epilepsy [13]. While network-based studies have been successful in delineating generic network properties, such as path length or clustering, additional work is needed in order to come to grips with the internal working of the systems underlying the network.

REVIEW INFO THEORY in resting state functional connectivity

In this paper we investigate the effects of aging in resting state functional connectivity nertworks using using a methodology that combines graph and information theoretic tools. In section 2 the methodology followed in the data acquisition, data preprocessing, anatomical parcellation and brain network reconstruction in two groups -24 young and 19 elder individuals- is presented. Then, we systematically study network robustness -functional network invariance under perturbation- is affected upon the removal of nodes in the functional connectivity network in resting state for both young and elder subjects. We provide a ranking of nodes that quantifies the impact of their obliteration using a network efficiency measure based on [14] that quantifies how the network efficiency in transmitting information deteriorates once a node is removed from the network. This is described in the results section 3. The paper concludes with a discussion section 4.

2 Materials and Methods

2.1 Subjects

Twenty-three healthy male volunteers (ages 21-32; mean 22.7) took part in the fMRI experiment. All subjects had normal or corrected-to-normal vision. The study was approved by the ethics committee of Okayama University, and written informed consent was obtained before the study.

2.2 Data acquisition

All subjects were imaged using a 1.5 T Philips scanner vision whole-body MRI system (Okayama University Hospital, Okayama, Japan), which was equipped with a head coil. Functional MR images were acquired during rest when subjects were instructed to keep their eyes closed and not to think of anything in particular. The imaging area consisted of 32 functional gradient-echo planar imaging (EPI) axial slices (voxel size=3x3x4 mm3, TR=3000 ms, TE=50 ms, FA=90^o, 64x64 matrix) that were used to obtain T2*-weighted fMRI images in the axial plane. We obtained 176 functional volumes and excluded the first 4 scans from analysis. Before the EPI scan, a T1-weighted 3D magnetization-prepared rapid acquisition gradient echo (MP-RAGE) sequence was acquired (TR=2300 ms, TE=2.98 ms, TI=900 ms, voxel size=1x1x1 mm3).

2.3 Data preprocessing

Data were preprocessed using Statistical Parametric Mapping software SPM8 [1] and REST v1.7 [2]. To correct for differences in slice acquisition time, all images were synchronized to the middle slice. Subsequently, images were spatially realigned to the first volume due to head motion. None of the subjects had head movements exceeding 2.5 mm on any axis or rotations greater than 2.5^o. After the correction, the imaging data were normalized to the Montreal Neurological Institute (MNI) EPI template supplied with SPM8 (resampled to 2x2x2 mm3 voxels) [3]. In order to avoid artificially introducing local spatial correlation, the normalized images were not smoothed. Finally, the resulting data were temporally band-pass filtered (0.01-0.08 Hz) to reduce the effects of low-frequency drifts and high-frequency physiological noises [15].

[1] http://www.fil.ion.ucl.ac.uk/spm/

[2] http://restfmri.net/forum/index.php

[3] http://imaging.mrc-cbu.cam.ac.uk/imaging/Templates

2.4 Anatomical parcellation

Before whole brain parcellation, several sources of spurious variance including the estimated head motion parameters, the global brain signal and the average time series in the cerebrospinal fluid and white matter regions were removed from the data through linear regression [**?**]. Then, the fMRI data were parcellated into 90 regions using an automated anatomical labeling template [**?**]. For each subject, the mean time series of each region was obtained by simply averaging the time series of all voxels within that region.

2.5 Brain network construction

To measure the functional connectivity among regions, we calculated the Pearson correlation coefficients between any possible pair of regional time series, and then obtained a temporal correlation matrix $(90x90)$ for each subject. We applied Fisher's r-to-z transformation to improve the normality of the correlation matrix. Then, two-tailed one-sample t-tests were performed for all the possible 4005 i.e., $\frac{90x89}{2}$ pairwise correlations across subjects to examine whether each inter-regional correlation significantly differed from zero.

A Bonferroni-corrected significance level of $P < 0.001$ was further used to threshold the correlation matrix into an adjacency matrix whose element was 1 if there was significant correlation between the two brain regions and 0 otherwise. Finally, an undirected binary graph was acquired in which nodes represent brain regions and edges represent links between regions. The study of the connectivity distribution of the resulting adjacency matrix is provided in the Appendix **??**.

2.6 Graph theoretic analysis

Until the recent advent of graph theoretic methods in R-fMRI, the focus was put on the identification of anatomically separated regions that show a high level of functional correlation during rest. The tools we use to model a system may also convey an ontological version of it, that is to say, the system under study is seen through the lens of a specific approach that necessarily shapes the observability domain. Thus, the identification of different subnetworks during rest can be seen as a by-product of the techniques used, for example identification component analysis (ICA) or clustering. Graph theory provides a theoretical framework to investigate the overall architecture of the brain. The use of graph theoretic techniques to model brain networks has shifted the emphasis from the identification of local subnetworks -default mode network, primary sensory motor network etc.- to the quantitative study of the topological and informational characteristics of large-scale brain networks. Graph theory-based approaches model the brain as a complex net-

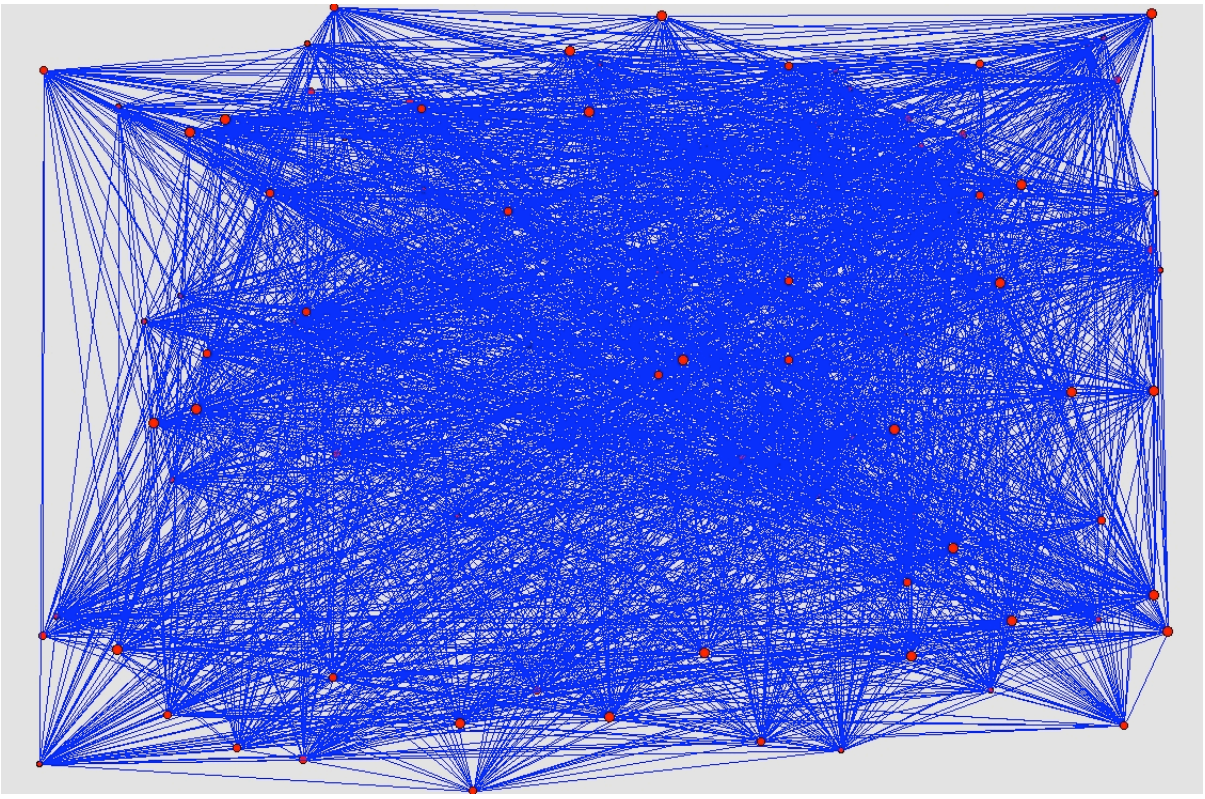

Fig. 1 Graphic representation of the functional connectivity among regions based on the temporal correlation matrix of the twenty-three healthy controls, using Pajek software [16]

work in which nodes represent brain regions of interest and the edges connecting nodes represent relationship between nodes e.g., functional connectivity.

The graph-based network provides a geometric representation to visualize brain connectivity patterns and an analytic toolbox to quantitatively characterize the overall topological organization. Graph-based techniques have proliferated in the last years providing new insights into the structure function relationship in the healthy brain, and in aging and neuropathological disorders [17], [18], [19]. Prove of the utility of this approach is that notable proponents of a modularist vision of brain connectivity to understand cognition, such as Gazzaniga [20] (see [21] for an early critic of the modularist approach and anticipating a shift toward a networks) has now embraced the complex brain networks approach to understand the interplay between structure and function in brain systems [22].

2.6.1 Network robustness, efficiency and node vulnerability

A critical aspect is to understand network robustness, that is, functional network invariance under perturbation. In essence, robustness measures the capacity of the network to perform the same function before and after a perturbation. Perturbations are events, internal or external, that elicit a change in the network configuration, as for example in, to obliterate a node or a change in the connectivity between nodes. Thus, for a given network $G(N,E)$ with an adjacency matrix A, a perturbation δ (e.g., the removal of a set of nodes M from N) transforms A into a new adjacency matrix A'. Thus, the initial graph $G(N,E)$ is transformed into a new post perturbation graph $G(N-M,E-E(M))$, where $E-E(M)$ is the set of edges that do not connect any of the deleted nodes in M. Now we want to calculate the robustness of the network to the perturbation δ. Robustness is here studied as a loss in the efficiency. Thus, the robustness measure, $\mathscr{R}$ for a network G is defined as the relative performance retained or efficiency loss under a network insult i.e., a perturbation δ, that transforms the initial network G into G^{δ}.

$$\mathscr{R}^{\delta}(G) = \frac{\Sigma(G^{\delta})}{\Sigma(G)} \tag{1}$$

Thus, from equation 1, a network G is considered to be robust (to a perturbation δ) if the network performance or efficiency $\Sigma(G)$ stays close to the original value after a perturbation, ideally $\mathscr{R}^{\delta} = 1$.

Now, we need to provide the formal definition of network efficiency. The efficiency of a network G, $\Sigma(G)$, is a network centrality measure that quantifies the network's reliability in transmitting information, once a node or a set of nodes have being removed. The network efficiency can be calculated using the Latora and Marchiori measure [14]. Accordingly, the efficiency in the communication between any two nodes in a graph G is equal to the inverse of the shortest path that connects them or $\varepsilon_{ij} = \frac{1}{d_{ij}}$. The efficiency of the graph is calculated as the average of the efficiency between any two nodes ε_{ij}

$$\Sigma(G) = \frac{\sum_{i \neq j \in G} \varepsilon_{ij}}{N(N-1)} = \frac{1}{N(N-1)} \frac{1}{\sum_{i \neq j \in G} d_{ij}} \tag{2}$$

where N is the number of nodes and d_{ij} is the shortest path length (the geodesic distance) between nodes i and j. According to equation 2, the quantity $\Sigma(G)$ is defined in the range $[0,1]$ and measures the mean flow-tare of information over G. Thus, a graph G with $\Sigma(G) = l$ is more efficient than a graph H with $\Sigma(H) = m$, if and only if $l > m$. Note that when there is no path that connects the nodes i and j, $d_{ij} = \infty$, and the efficiency in the communication of the two nodes is zero, $\varepsilon_{ij} = 0$.

The global network efficiency is 0.3678 for young subjects and 0.1144 for elder subjects. Thus, young subjects connectivity network is three times more efficient in terms of the shortest path distance between any two nodes.

We can, in addition to robustness and efficiency of G calculate the information centrality C of any node i in the network G as the variation in the network efficiency caused by the removal of the edges incident in i. The centrality of a node i C_i is calculated as the difference between the efficiency of the original graph G with N nodes and E edges , G(N,E), and the efficiency of the resulting graph G_i with N nodes and $E - k_i$ edges. Thus, the centrality of a node is a normalized measure of the loss in network efficiency caused by the isolation of a node in G.

$$C_i = \frac{\Sigma(G(N,E)) - \Sigma(G(N,E-k_i))}{\Sigma(G(N,E))} \tag{3}$$

By the same token, the information centrality of a set of nodes S can be calculated as normalized measure of the loss in network efficiency caused by the isolation of a set of nodes S in G.

$$C_S = \frac{\Sigma(G(N,E)) - \Sigma(G(N,E-k_S))}{\Sigma(G(N,E))} \tag{4}$$

In Table **??** (see Excel file) is shown the information centrality for each of the AAL regions.

2.7 Information theoretic analysis on Markov chains

The undirected binary graph depicted in Figure 1 is the geometric characterisation of the adjacency matrix A, in which $a_{ij} = 1$ if AAL region i and AAL region j show a significant correlation, and $a_{ij} = 0$ otherwise. We transform the binary adjacency matrix A into a weighted adjacency matrix T, where $T_{ij} = \frac{a_{ij}}{\sum_j a_{ij}}$. Thus, the new graph has the same number of nodes and the weight connecting any two nodes is T_{ij}. Note that $T_{ij} = 0$ if nodes are not connected, symmetry is preserved $T_{ij} = T_{ji}$.

Now, let us consider a random walk -a particle moving from node to node- on the weighted undirected graph T. A random walk $\{X_1 \dots X_n\}$ is defined as the list of nodes visited by the particle. The probability that the particle moves from i to j is given by T_{ij}. This stochastic process defines a Markov chain because the probability that the particle moves from state n to state $n+1$ is independent of the previous states, that is, $P(X_{n+1} = x_{n+1}|X_n = x_n) = P(X_{n+1} = x_{n+1}|X_n = x_n, X_{n-1} = x_{n-1}, \dots, X_1 = x_1)$.

The stationary distribution of the random walk on the undirected graph is $\mu = \{\frac{k_1}{2E}, \frac{k_2}{2E}, \dots, \frac{k_N}{2E}\}$, where k_i is the connectivity degree of node i and E is the total number of links contained in the graph. It ought to be noted that the stationary distribution does not depend on the number of nodes, but only on the total number of links E, and the weight (or the number) of links connecting each node. Thus, the stationary distribution holds the local property that it is not altered by changes in the weights of non neighbors nodes, while keeping the total weight of the graph constant.

The entropy rate of a stochastic process represents the rate at which the entropy of a sequence e.g., a random walk, grows with n. Formally, for the stochastic process $\mathscr{X} = \{X_1, \ldots, X_n\}$ the entropy rate is given by

$$H(\mathscr{X}) = \lim_{n\to\infty} \frac{1}{n} H(X_1, X_2, \ldots, X_n) \tag{5}$$

For a stationary Markov chain, the entropy rate is

$$H(\mathscr{X}) = \lim_{n\to\infty} H(X_n|\, X_{n-1}, \ldots, X_1) = \lim_{n\to\infty} H(X_n|X_{n-1}) = \lim_{n\to\infty} H(X_2|X_1) \tag{6}$$

We define a Markov process for both the young subjects and the elder ones with their transition matrix given by T^y_{ij} and T^e_{ij} respectively

$$\begin{aligned} T^y_{ij} &= \frac{A^y_{ij}}{\sum_j A^y_{ij}} \\ T^e_{ij} &= \frac{A^e_{ij}}{\sum_j A^e_{ij}} \end{aligned} \tag{7}$$

where A^y_{ij} and A^e_{ij} are the binary adjacency matrix of the young and the elder subjects. Thus, the entropy rate is

$$\begin{aligned} H(\mathscr{X}^y) &= -\sum_{ij} \mu^y_i T^y_{ij} \log T^y_{ij} \\ H(\mathscr{X}^e) &= -\sum_{ij} \mu^e_i T^e_{ij} \log T^e_{ij} \end{aligned} \tag{8}$$

We calculate the entropy rate for the resulting Markov process after having removed all the edges incident to a node i $\mathscr{X}_i$. Thus, the transition matrix T' for the Markov process $\mathscr{X}_i$ is such that $T' = T$ except for both the column and row i which are all 0, $T'_{i,} = T'_{,i} = 0$. The relative entropy of this new stochastic process $\mathscr{X}_i$ is:

$$H(\mathscr{X}_i) = -\sum_{k,j,k\neq i} \mu_k T'_{kj} \log T'_{kj} \tag{9}$$

By the same token, the entropy rate when the edges incident to any of the nodes of the components of the set of nodes S are removed is

$$H(\mathscr{X}_S) = -\sum_{k,j,k\neq S} \mu_k T'_{kj} \log T'_{kj} \tag{10}$$

Analogously to the information centrality C_i defined in 3, we calculate the normalized value D_i defined as the difference between the entropy rate of the original Markov process, $\mathscr{X}$, and the resulting process of deleting the edges incident in i, $\mathscr{X}_i$.

$$D_i = \frac{H(\mathscr{X}) - H(\mathscr{X}_i)}{H(\mathscr{X})} \tag{11}$$

By the same token, when the resulting Markov process is given by the removal of the edges incident in any of the nodes in a set S $\mathscr{X}_S$ we have

$$D_S = \frac{H(\mathscr{X}) - H(\mathscr{X}_S)}{H(\mathscr{X})} \tag{12}$$

JAIME: TO DO

3 Results

We have analyzed the functional connectivity in resting state of both young and elder individuals. The nodes representing the ninety brain regions based on the AAL parcelation have been ranked in terms of their impact in terms of network robustness upon removal. Interestingly we find that in both elder and young groups the removal of certain nodes does not necessarily triggers a decrease in network robustness, the obliteration of certain nodes may also produces a positive impact in the network function, increasing the network robustness when the node is removed. We study network robustness based on the new network efficiency/performance measure (equation 2) to investigate the network functionality when a set of nodes are obliterated. The results show that in young subjects, the nodes with a positive impact are ... TO DO LI/JAIME compared with elder subjects ... TO DO LI/JAIME.

In the second part we use information-theoretic measures to study the impact of the removal of nodes in the network. First, we model the network flows in terms of a stationary Markov chain which describes how a particle walks randomly from node to node, in both the young and elder functional connectivity graph. The probability transition matrix is derived from the binary adjacency matrix using the local property of connectivity degree. The entropy rate of a random walk on a graph in which a node or group of nodes has been removed is calculated.

The results show that in young subjects, after he removal of the nodes with a positive impact the entropy rate is $><$? TO DO JAIME than in the case of elder subjects.

4 Discussion

References

1. M. E. Raichle and D. A. Gusnard, "Intrinsic brain activity sets the stage for expression of motivated behavior," *The Journal of Comparative Neurology*, vol. 493, no. 1, pp. 167–176, 2005.
2. P. Fransson, "How default is the default mode of brain function?: Further evidence from intrinsic BOLD signal fluctuations," *Neuropsychologia*, vol. 44, no. 14, pp. 2836–2845, 2006.

3. S.-M. Kokkonen, J. Nikkinen, J. Remes, J. Kantola, T. Starck, M. Haapea, J. Tuominen, O. Tervonen, and V. Kiviniemi, "Preoperative localization of the sensorimotor area using independent component analysis of resting-state fMRI," *Magnetic resonance imaging*, vol. 27, pp. 733–740, July 2009. PMID: 19110394.
4. J. S. Damoiseaux, S. A. R. B. Rombouts, F. Barkhof, P. Scheltens, C. J. Stam, S. M. Smith, and C. F. Beckmann, "Consistent resting-state networks across healthy subjects," *Proceedings of the National Academy of Sciences of the United States of America*, vol. 103, pp. 13848–13853, Sept. 2006. PMID: 16945915.
5. M. Hampson, B. S. Peterson, P. Skudlarski, J. C. Gatenby, and J. C. Gore, "Detection of functional connectivity using temporal correlations in MR images," *Human brain mapping*, vol. 15, pp. 247–262, Apr. 2002. PMID: 11835612.
6. M. D. Hunter, S. B. Eickhoff, T. W. R. Miller, T. F. D. Farrow, I. D. Wilkinson, and P. W. R. Woodruff, "Neural activity in speech-sensitive auditory cortex during silence," *Proceedings of the National Academy of Sciences of the United States of America*, vol. 103, pp. 189–194, Jan. 2006. PMID: 16371474.
7. M. D. Fox, M. Corbetta, A. Z. Snyder, J. L. Vincent, and M. E. Raichle, "Spontaneous neuronal activity distinguishes human dorsal and ventral attention systems," *Proceedings of the National Academy of Sciences of the United States of America*, vol. 103, pp. 10046–10051, June 2006. PMID: 16788060.
8. J. L. Vincent, I. Kahn, A. Z. Snyder, M. E. Raichle, and R. L. Buckner, "Evidence for a frontoparietal control system revealed by intrinsic functional connectivity," *Journal of neurophysiology*, vol. 100, pp. 3328–3342, Dec. 2008. PMID: 18799601.
9. D. Watts and S. Strogatz, "Collective dynamics of 'small-world' networks," *Nature*, vol. 393, pp. 244–442, 1998.
10. D. S. Bassett and E. Bullmore, "Small-world brain networks," *The Neuroscientist*, vol. 12, pp. 512–523, Dec. 2006.
11. K. Supekar, V. Menon, D. Rubin, M. Musen, and M. D. Greicius, "Network analysis of intrinsic functional brain connectivity in alzheimer's disease," *PLoS Computational Biology*, vol. 4, June 2008. PMID: 18584043 PMCID: PMC2435273.
12. Y. Liu, M. Liang, Y. Zhou, Y. He, Y. Hao, M. Song, C. Yu, H. Liu, Z. Liu, and T. Jiang, "Disrupted small-world networks in schizophrenia," *Brain: a journal of neurology*, vol. 131, pp. 945–961, Apr. 2008. PMID: 18299296.
13. W. Liao, Z. Zhang, Z. Pan, D. Mantini, J. Ding, X. Duan, C. Luo, G. Lu, and H. Chen, "Altered functional connectivity and small-world in mesial temporal lobe epilepsy," *PLoS ONE*, vol. 5, p. e8525, Jan. 2010.
14. V. Latora and M. Marchiori, "Efficient behavior of small-world networks," *Physical Review Letters*, vol. 87, p. 198701, Oct. 2001.
15. Q. Jiao, G. Lu, Z. Zhang, Y. Zhong, Z. Wang, Y. Guo, K. Li, M. Ding, and Y. Liu, "Granger causal influence predicts BOLD activity levels in the default mode network," *Human Brain Mapping*, vol. 32, no. 1, pp. 154–161, 2011.
16. V. Batagelj and A. Mrvar, "Pajek - analysis and visualization of large networks," in *Graph Drawing Software* (M. Jünger and P. Mutzel, eds.), Mathematics and Visualization, pp. 77–103, Springer Berlin Heidelberg, Jan. 2004.
17. D. A. Fair, A. L. Cohen, J. D. Power, N. U. F. Dosenbach, J. A. Church, F. M. Miezin, B. L. Schlaggar, and S. E. Petersen, "Functional brain networks develop from a "local to distributed" organization," *PLoS computational biology*, vol. 5, p. e1000381, May 2009. PMID: 19412534.
18. J. Wang, X. Zuo, and Y. He, "Graph-based network analysis of resting-state functional MRI," *Frontiers in systems neuroscience*, vol. 4, p. 16, 2010. PMID: 20589099.
19. Y. He and A. Evans, "Graph theoretical modeling of brain connectivity," *Current opinion in neurology*, vol. 23, pp. 341–350, Aug. 2010. PMID: 20581686.
20. M. S. Gazzaniga, ed., *The New Cognitive Neurosciences: Second Edition*. The MIT Press, 2 ed., Nov. 1999.
21. J. Fuster, "The module: crisis of a paradigm book review, "the new cognitive neurosciences" 2nd edition, m.s. gazzaniga, editor-in-chief, mit press," *Neuron*, no. 26, pp. 51–53, 2000.

22. D. S. Bassett and M. S. Gazzaniga, "Understanding complexity in the human brain," *Trends in cognitive sciences*, vol. 15, pp. 200–209, May 2011. PMID: 21497128.